Article

Glycosylated RAFT polymers with varying PEG linkers produce different siRNA uptake, gene silencing and toxicity profiles

Elizabeth G.L. Williams, Oliver Earl Hutt, Tracey M. Hinton, Sophie C Larnaudie, Tam Le, James M. MacDonald, Pathiraja Gunatillake, San H. Thang, and Peter J Duggan

Biomacromolecules, **Just Accepted Manuscript** • DOI: 10.1021/acs.biomac.7b01168 • Publication Date (Web): 23 Oct 2017

Glycosylated RAFT polymers with varying PEG linkers produce different siRNA uptake, gene silencing and toxicity profiles

Elizabeth G. L. Williams,[a‡] Oliver E. Hutt,[a‡] Tracey M. Hinton,[b] Sophie C. Larnaudie,[a‡] Tam Le,[a] James M. MacDonald,[a] Pathiraja Gunatillake,[a] San H. Thang,[a] Peter J. Duggan[a,c]*

[a] CSIRO Manufacturing, Private Bag 10, Clayton South, VIC, 3169, Australia.

[b] CSIRO Health and Biosecurity, Port Arlington Rd, East Geelong, VIC 3219, Australia.

[c] School of Chemical and Physical Sciences, Flinders University, Adelaide, South Australia, 5042, Australia.

Supporting Information

The following files are available free of charge.

^{1}H and ^{13}C NMR data for sugar-PEG-azide click precursors **18**, **19**, **20**, **30** and **31**, ABA triblock **11**, and clicked polymers **32**, **33**, **34**, **35** and **36** (PDF)).

AUTHOR INFORMATION

* Corresponding author: Oliver Hutt, Email: oliver.hutt@csiro.au

Author Contributions The manuscript was written through contributions of all authors. All authors have given approval of the final version of the manuscript. ‡These authors contributed equally.

ABSTRACT

Achieving efficient and targeted delivery of short interfering (siRNA) is an important research challenge to overcome to render highly promising siRNA therapies clinically successful. Challenges exist in designing synthetic carriers for these RNAi constructs that

provide protection against serum degradation, extended blood retention times, effective cellular uptake through a variety of uptake mechanisms, endosomal escape and efficient cargo release. These challenges have resulted in a significant body of research, and led to many important findings about the chemical composition and structural layout of the delivery vector for optimal gene silencing. The challenge of targeted delivery vectors remains, and strategies to take advantage of nature's self-selective cellular uptake mechanisms for specific organ cells, such as the liver, have enabled researchers to step closer to achieving this goal. In this work we report the design, synthesis and biological evaluation of a novel polymeric delivery vector, incorporating galactose moieties to target hepatic cells through clathrin-mediated endocytosis at asialoglycoprotein receptors. An investigation into the density of carbohydrate functionality and their distance from the polymer backbone is conducted using Reversible Addition Fragmentation chain Transfer (RAFT) polymerisation and post-polymerisation modification.

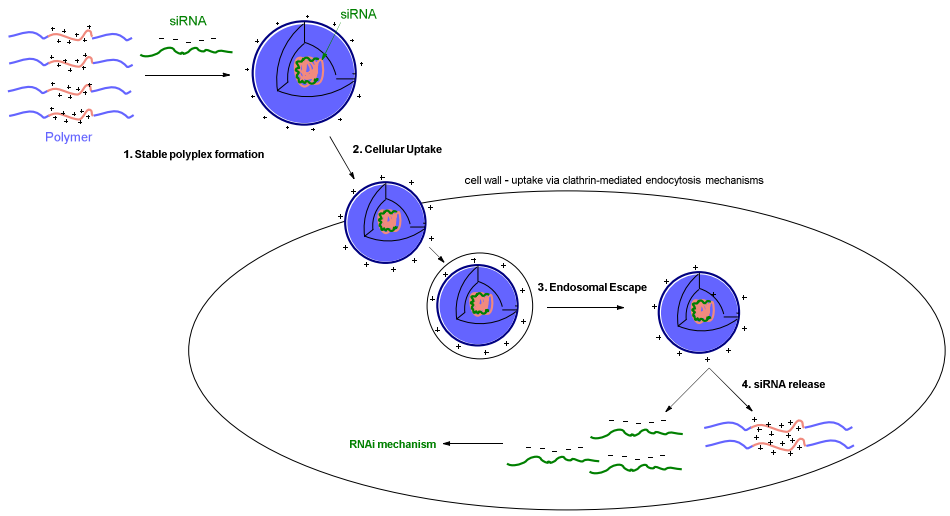

INTRODUCTION

In recent years, many disease interventions have focussed on the naturally occurring RNA interference mechanism, which consists of specific gene suppression by the action of small

interfering RNA (siRNA) chains.[1] The basis of this approach is the delivery of artificial exogenous siRNA to cells to knock-down targeted genes.[2] As such, siRNA could be used in the treatment of genetic disorders[3], in cancer therapy,[4] or as antivirals.[5] However, the strong negative charge and instability of naked RNA *in vivo* [6] requires a suitable carrier for these siRNAs. Viral carriers are easy to develop, but present problems such as immunogenicity or oncogenicity, low nucleic acid loading capacity and limited control over the type of cells that is transduced.[7-8] Therefore, siRNA delivery has become a very active field of research.[9]

The liver is an important target for RNAi-based therapies due to its role in the production and secretion of serum proteins into the blood, potentially enabling a permanent therapeutic response.[10] The present study focuses on interventions for viral liver diseases (such as hepatitis A, B, C and E) and seeks to couple a polymeric siRNA delivery vehicle with a targeting strategy to take advantage of the presence of asialoglycoprotein receptors (ASGP-R) on mammalian liver cells.[11]

The asialoglycoprotein receptor (ASGPR) is a member of the large family of Ca^{2+}-dependent lectins (C-type lectins) present in hepatocytes that remove desialylated proteins from the blood serum. The ASGPRs recognise and clear glycoproteins with either terminal galactose (Gal) or N-acetyl galactosamine (GalNAc) through activation of clathrin-mediated endocytosis. Upon encapsulation, the decrease in pH in the endosomal compartment is sufficient to break the carbohydrate-receptor interaction and the ASCGR is ultimately returned to the surface within 15 minutes (Fig. 1).

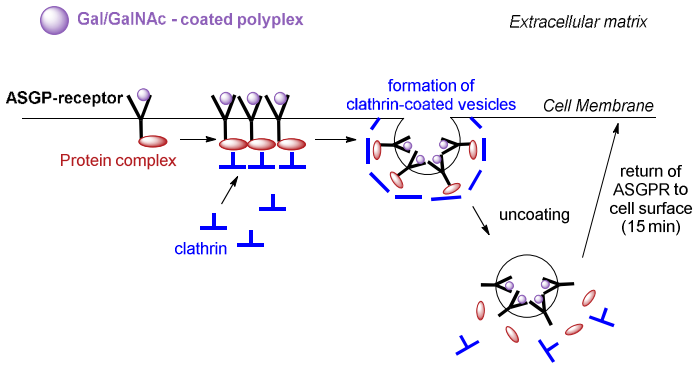

Figure. 1: Clathrin-mediated endocytosis, triggered by binding of Gal or GalNAc ligands at the ASGP receptor.

The high level of expression of ASGPR in the liver and it's specificity for Gal and GalNAc hasled to the successful exploitation of this naturally occurring mechanism to target therapies, including small-molecule cytotoxics for hepatic cancer. For example, the GalNAc-Doxorubicin-HPMA copolymers reported by Kopeček *et al* are retained in the human liver for more than 24 hours compared with controls (Fig. 2A).[12] Incorporation of enzymatically cleavable tetrapeptide units enabled the targeted delivery of doxorubicin.

GalNAc-siRNA conjugates developed by Alnylam also effectively target the liver and are effective in targeting the genes involved in range of diseases including transthyretin-related amlyoidosis, hemophilia, and porhyria (Fig. 2B).[13] These tri-antennary GalNAc recognition elements were specifically designed to be 15-20 Å apart, within a tripod, to mimic the triangular spatial arrangement of hepatic ASGP receptors, thereby maximising ligand recognition and cellular uptake.[14] Similarly, GalNAc-siRNA dynamic polyconjugates, which rely on a reversible succinimide-amide linkage, have shown efficacy against hepatitis B (Figure 2C)[15]. More recently, a tetradentate GalNAc targeting group was also reported for ASGPR (Figure 2D)[16].

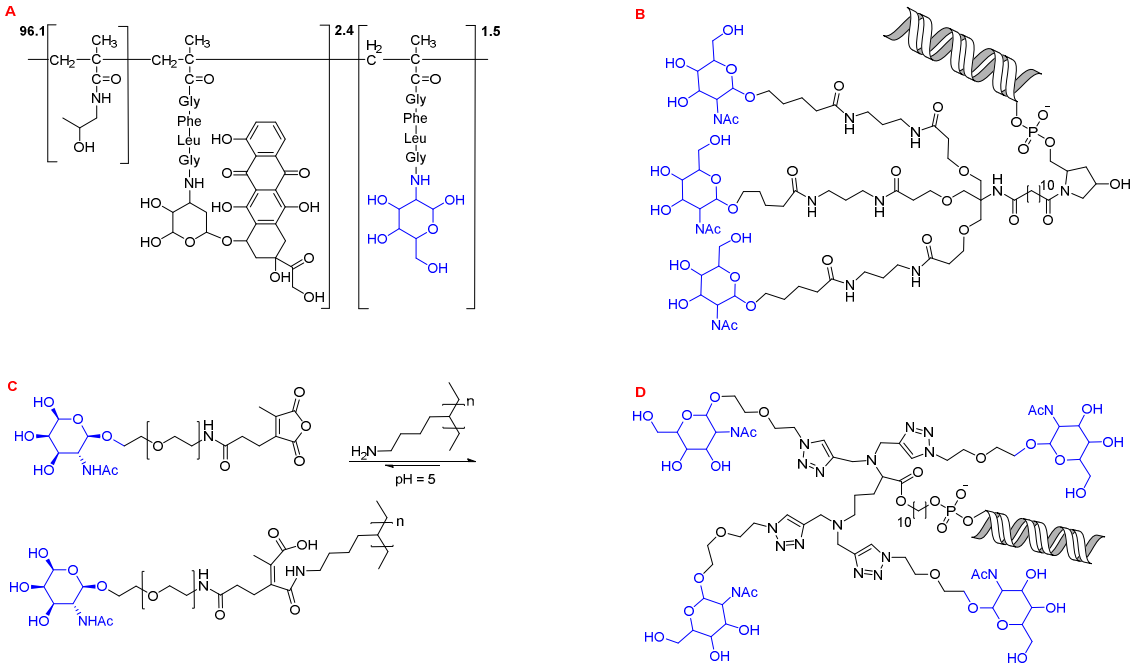

Figure 2. Asiaglycoprotein receptor targeting therapeutic delivery systems.

Whilst tri-antennary based GalNAc vectors have shown a much stronger affinity to ASGPR compared to monovalent vectors, based on IC_{50} values, they often require a complex synthesis.[17-18] With the aim of developing synthetically simple delivery vectors, the Reineke group have reported an AB diblock copolymer comprising a GalNAc-functionalised 2-hydroxyethyl methacrylamide (HEMAA) and 2-aminoethyl methacrylamide (AEMA) monomers (Fig. 3) for the delivery of nanomedicine formulations, including plasmid DNA, to the liver[19]. This delivery system incorporates a cationic block (AEMA), allowing the RNAi-based therapeutics to associate with the carrier polymer via an electrostatic interaction, rather than the covalent delivery vectors designed by Alnylam. By using the Reversible Addition-Fragmentation Chain Transfer (RAFT) – a controlled free radical polymerisation process,[8] Reineke and colleagues were able to interrogate optimum cationic carrier block length, whilst

keeping the targeting GalNAc block constant (Fig. 3A). A glucose control (Fig. 3B) was also synthesised to evaluate targeting effects of the GalNAc polymers.

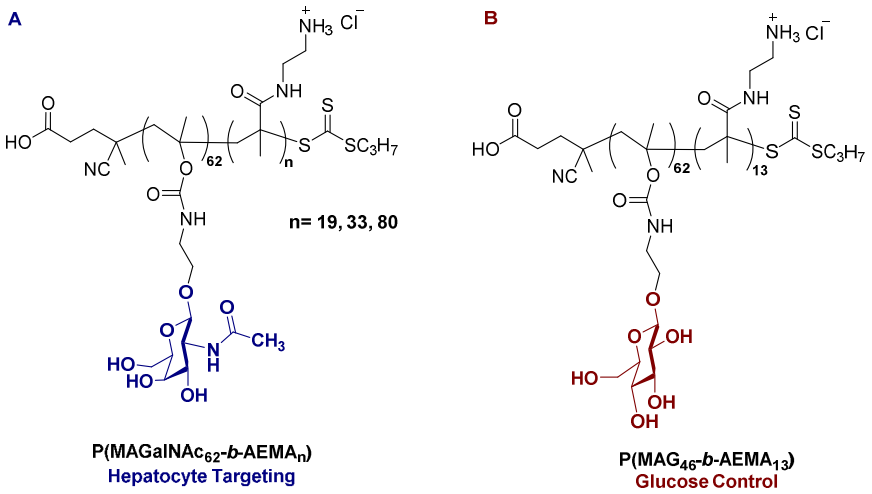

Figure 3: GalNAc and Glucose containing RAFT polymers prepared by the Reineke group.

ASGP-R are carbohydrate-binding proteins (lectins) that bind β-galactose, and galactosylated polymers have been reported to show good hepatocyte specificity and higher transfection efficiency than non galactose-containing polymers.[20]

The multivalent GalNAc copolymers were found to provide stronger interactions with ASGPRs at 5 orders of magnitude greater than monomeric GalNAc. The polymers were assayed against HepG2 cells, derived from human hepatocellular carcinoma, and HeLa cells, derived from human cervical adenocarcinoma. Lower HepG2 cell viability was observed for the GalNAc-containing polymers at N:P (nitrogen (Polymer): phosphate (siRNA backbone)) ratios of 2.5 and 5. Transgene expression using gWiz-luc plasmid polyplexes in HepG2 and HeLa cells showed that GalNAc containing polymers promoted higher cellular uptake and therefore transgene expression in HepG2 cells than in HeLa cells due to the presence of the ASGP-receptors on HepG2 cells. However, MAG-containing control polymers show similar levels of gene expression in HeLa cells compared to HepG2 cells, and efficient gene delivery

is seen even at low N:P ratios. This result suggests that the cationic copolymer block or excess free polymer may promote nonspecific cell surface interactions and non-ligand dependent uptake mechanisms, in addition to the ASGPR-mediated uptake promoted by the GalNAc block. Following tail-vein injection of fluorescently labelled p(MAGalNAc$_{62}$-*b*-AEMA$_{33}$) and p(MAG$_{46}$-*b*-AEMA$_{13}$) pDNA polyplexes, total fluorescence in all harvested tissues (harvested 30 min post-injection) was measured to determine the biodistribution of the two vectors. p(MAGalNAc$_{62}$-*b*-AEMA$_{33}$) was found mainly in the liver, accounting for 80% of total injected fluorescence, whilst p(MAG$_{46}$-*b*-AEMA$_{13}$) displayed 64% of total fluorescence in the liver, with 20% of fluorescence accounted for by polymer in the kidneys. Collectively, the *in vitro* and *in vivo* results show that the MAGalNAc polymer does provide some targeting to the liver above the glucose control, however, the majority of the retention is due to other MAGalNAc-independent cellular uptake mechanisms.

Narain and co-workers also used a RAFT di-block copolymer approach incorporating a cationic AEMA segment and an asialoglycoprotein targeting 2-lactobionoamidoethyl methacrylamide (LAEMA) segment (Fig. 4)[21]. Statistical copolymers were also synthesised to understand toxicity profiles of concentrated cationic segments compared to the random spread of these functionalities. These polymer vectors were used to condense DNA (β-galactosidase plasmid) rather than siRNA, with a focus on transfection to HepG2 cells for the treatment of hepatocellular carcinoma.

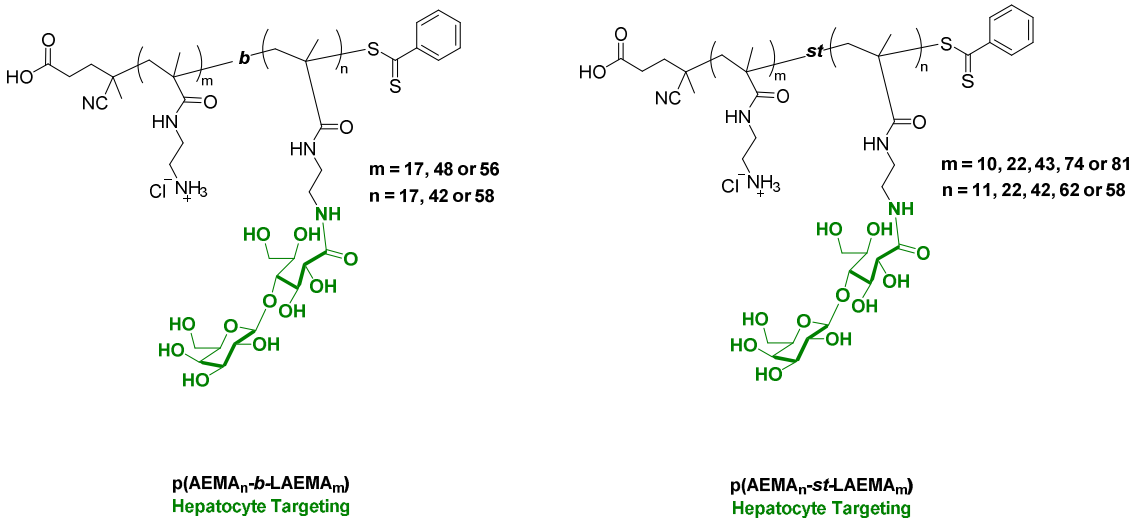

Figure 4: Lactobionic-containing block and statistical copolymers for targeting DNA plasmid delivery to HepG2 and Huh7.5 cells *via* endocytosis through the ASGP-R.

Their studies found that toxicity decreased (obtained by MTT assay in HepG2 cells) with increasing carbohydrate content, which is expected due to lower toxic cationic content. However, block copolymers were found to be more toxic than their statistical counterparts, even when a higher carbohydrate content is incorporated into the diblock copolymer. This was attributed to the inability of the block copolymer to mask the toxic cationic components. When complexed with β-galactosidase plasmid, the resulting polyplexes were stable at N/P ratios of between 48-65. Zeta potentials of the block copolymers was found to be close to zero, proving that the condensed DNA is mostly held within the core of the polyplex, whilst the statistical copolymer polyplexes had net positive zeta potentials. Block copolymer polyplexes also exhibited smaller sized complexes by dynamic light scattering (DLS) and therefore able to condense DNA more efficiently into the polyplex core, compared to their statistical counterparts. When HepG2 and Huh 7.5 cells were treated with these polyplexes, higher molecular weight polymers provided improved transfection, however these were also more toxic, proving that a careful balance of cationic charge and carbohydrate ratio, and the

appropriate molecular weight must be struck for efficient transfection. DNA transfection was higher in HepG2 cells than in Huh7.5 cells, particularly when comparing p($AEMA_{58}$-b-$LAEMA_{56}$). When evaluated in hepatic cells lines that do not express ASGPR's on their surface (HeLa and SK hep 1), these polyplexes exhibit limited transfection: 25 U/mg in SK hep 1 compared to 80 U/mg in HepG2 for p($AEMA_{81}$-st-$LAEMA_{58}$), proving uptake via ASGPR-mediated endocytosis. To confirm this finding, a competitive uptake study using free asialofetuin was conducted. Asialofetuin did not prevent transfection completely, which was attributed to higher multiples of galactose molecules on the surface of the polyplexes of the block copolymer complexes, enabling higher binding affinity, despite competition from asialofetuin. Confocal studies of Cy3-labeled plasmid to identify uptake in the presence and absence of asialofetuin. The high transfection efficiency of the nearly neutral p($AEMA_{58}$-b-$LAEMA^{56}$) polyplex suggests that the distances between the galactose residues are optimal in this complex, consistent with the 'cluster effect' identified by Lee *et al*[17, 22].

Narain and co-workers recently reported a novel polyplex formulation that exhibited improved complexation with siRNA for the down regulation of the epidermal growth factor receptor (EGFR) proteins in cervical cancer cells[23]. By combining an oxazoborole-functionalised monomers with *N*-isopropyl acrylamide (NIPAM) copolymer as a stimuli-responsive protective system; and a glycopolymer containing cationic residues for siRNA complexation, cross-linking between the oxazoborole and diols of the glycopolymer enable a stable polyplex to be formed. This system exhibited gene silencing of up to 60% in HeLa (cervical) cancer cells with low toxicity. This approach is particularly novel given the use of two complimentary polymers to provide specific roles within the siRNA delivery and release process. The targeting lactobionic functionalities were incorporated in a statistical copolymer, and therefore the effect of spacing and density was not investigated. Nonetheless, the

polyplex has shown impressive results and is a promising avenue of further investigation for oxazoborole-containing polymers.

Whilst distance between targeting groups is important, another factor to take into consideration while establishing the synthetic strategy is the density of targeting moieties on the polymer chains. Some results have indeed shown that density matters for efficient recognition by ASGP-R and cell internalization:[24] if the density of targeting groups is too low they might not be able to bind the receptors and if it is too high, steric hindrance problems might be encountered. For similar reasons, the length of the spacers between the polymer backbone and the targeting group also has to be considered and optimized.

In light of these results, it is reasonable to consider incorporating the triangular spatial arrangement of Alnylam's hepatic ASGP receptors into a polymer structure to obtain improved performance in a polymer context. We postulated that having a more accessible targeting moiety, further removed from the polymer backbone may further promote ASGPR-mediated uptake.

We have decided to focus primarily on polymeric materials. From a biological point of view, the structure of the chosen polymeric carrier has to be very precisely controlled.[25] This control is possible by polymerization processes such as Reversible Addition-Fragmentation chain Transfer (RAFT) (Figure 4, which enable the fabrication of controlled molecular weight and polymers with very narrow polydispersity.[26-28] The RAFT process is a living free radical polymerization process which uses a chain transfer agent (CTA), typically a thiocarbonylthio compound, to perform the radical exchange between propagating and dormant species.

To be an efficient siRNA delivery vector, the chosen carrier has to meet a number of requirements. The vector has to be hydrophilic and non-cytotoxic, it should bind the siRNA

strongly enough to protect it from degradation, but release it, and enable gene silencing upon cellular uptake.[8] Our team has recently synthesised an ABA triblock polymer constituted of a cationic core of 110 units of *N,N*-dimethylaminoethyl methacrylate (DMAEMA) and hydrophilic 25-units outer blocks made of polyethyleneglycol methacrylate (PEGMA) (Figure 4). This delivery vector has shown 75% gene silencing on the tested cell lines and also good serum stability and toxicity profiles.[29] Given this success we were interested in installing ASGPR targeting groups into the outer block in order to target siRNA delivery to the liver.

In order to achieve and understand the effect of installing ASGPR targeting moieties into a polymeric ABA-triblock delivery vehicle, three main parameters must be correlated. The nature of the targeting group, the length of the linker between the polymer backbone and the target group, and the brush density (i.e., the number) of the targeting groups per polymer chain.[24] However, the above requirements are difficult to combine with the inherent batch-to-batch variation of any given polymerization process. Although it can be argued that the variation is relatively minor, it is still sufficient to engender doubt into the interpretation of biological results when comparing multiple polymers across a series.

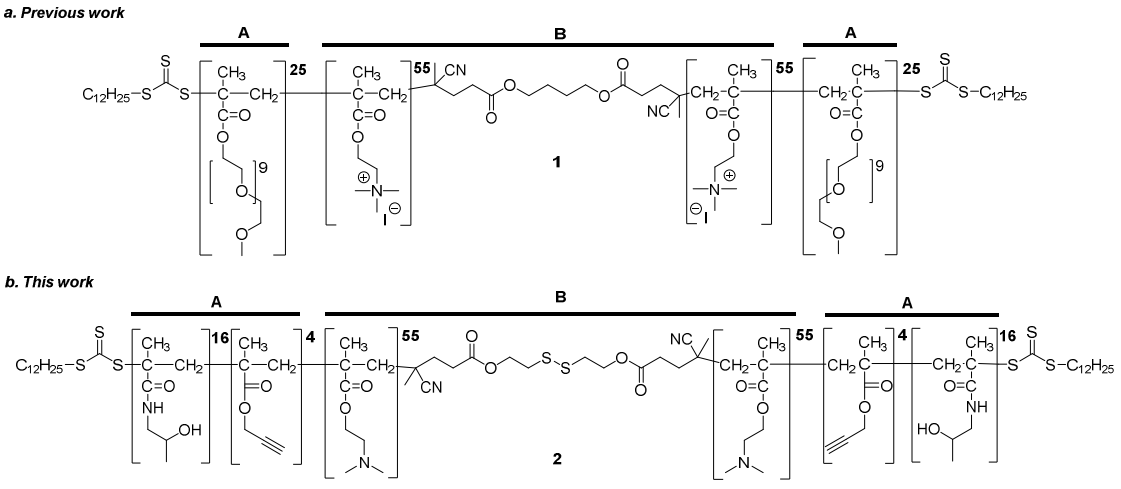

Figure 5: a. $(OEGMA\ 475)_a$-$(DMAEMA)_b$ ABA-triblock copolymer previously reported to achieve 75% knockdown. b. New $(PEGMA\text{-}HPMA)_a$-$(DMAEMA)_b$ ABA-triblock copolymer reported here.

In this light, post-polymerisation modification of a single polymer scaffold has emerged as a strategy to address the batch-to-batch polymerisation variation. Using this approach a library of polymers can be accessed from a single batch of well-defined polymer. Here we report the synthesis a biodegradable *bis*-RAFT agent and its subsequent use to synthesise a polymeric ABA-triblock co-polymer **2** made of an *N*-(2-hydroxypropyl)methacrylamide (HPMA), propargyl methacrylate (PgMA) and DMAEMA (Fig.5b). We also describe the synthesis of azide-bearing polyethylene glycol (PEG) linked galactose targeting agents and corresponding glucose controls and the grafting of these groups onto the polymer backbone with the copper-catalysed azide-alkyne cycloaddition (CuAAC, "click" reaction)[30-33]. Finally, we report our biological results, including effect of PEG linker length, and the efficacy of the PEG-linked galactose moiety as targeting unit for the ASGPR receptor.

EXPERIMENTAL SECTION

General Experimental: N,N-dimethylaminoethyl methacrylate (DMAEMA) and N-(2-Hydroxypropyl) methacrylamide (HPMA) monomers were purchased from Aldrich and purified by stirring in the presence of inhibitor-remover for hydroquinone or hydroquinone monomethyl ether (Aldrich, catalogue number 311332) for 30 min prior to use. 1,10-Azobis(cyclohexanecarbonitrile) (VAZO-88) and azobisisobutyronitrile (AIBN) initiator (DuPont) were used as received. Dichloromethane (DCM), n-heptane, diisopropyl ether, diethyl ether, pentane, propargyl bromide, methyl iodide, methanol, and other chemical substances were commercial reagents and used without further purification. 1H and 13C NMR (400 MHz) spectra were recorded using a Bruker Av400 spectrometer at 25°C.

Chemical shifts are reported in ppm downfield from tetramethylsilane (TMS, 0 ppm). The following abbreviations were used to explain the multiplicities: s = singlet, d = doublet, t = triplet, dd = doublet of doublets, dq = doublet of quadruplets, bs = broad singlet, m = multiplet. For carbon NMR, all peaks correspond to one carbon, unless specified. M(th) refers to the theoretical molecular weight based on monomer conversion, M(NMR) to the calculated molecular weight based on relative integration of signals corresponding to the different units. Mass spectrometric analyses were performed on a Thermo Scientific Q Exactive mass spectrometer fitted with a HESI ion source. Positive and negative ions were recorded in an appropriate mass range at 140,000 mass resolution. The probe was used with 0.6ml/min flow of solvent (usually methanol), and a solution of Reserpine was also introduced into the probe during the experiments to serve as a lock mass in both positive and negative ion modes. The nitrogen nebulizing/desolvation gas used for vaporization was heated to 100°C in these experiments. The sheath gas flow rate was set to 25 and the auxiliary gas flow rate to 7 (both arbitrary units). The spray voltage was 3.8 kV and the capillary temperature was 300°C. FTIR spectra were obtained using a Thermo Nicolet 6700 spectrometer using a SmartATR (attenuated total reflectance) attachment fitted with a diamond window. Gel permeation chromatography (GPC) measurements were performed on two different sets of equipment. The first used a Shimadzu system equipped with a CMB-20A controller system, a SIL-20A HT autosampler, a LC-20AT tandem pump system, a DGU-20A degasser unit, a CTO-20AC column oven, a RDI-10A refractive index detector and 4 × Waters Styragel columns (HT2, HT3, HT4, HT5 each 300 mm × 7.8 mm providing an effective molar mass range of 100 – 4 × 106). This GPC system used *N,N*-dimethylacetamide (DMAc) (with 2.1 g L–1 of lithium chloride (LiCl)) as eluent with a flow rate of 1 mL/min at 80°C. The molecular weights reported are relative to linear poly(methyl methacrylate) (PMMA) standards. The second GPC apparatus was an Agilent SECcurity

GPC system (1200 series), comprising a quaternary pump (G1311B), a solvent degasser (G1379B), an autosampler (G1329B), a refractive index detector (G1362) at 35 °C and a temperature controlling unit (G1316A). The temperature controller unit housed three Eprogen, Inc. CATSEC columns (250 × 4.6 mm) (CCS201-25 5µ 100 Å, CCS203-25 5µ 300 Å, and CCS210-25 7µ 1000 Å) and an Eprogen, Inc. CATSEC guard column (50 × 4.6 mm) (FCCS210-5 7µ 1000 Å) at 25 °C. This system uses an eluent of 1 wt % acetic acid/0.10 M Na2SO4 (aqueous) at a flow rate of 0.3 mL min–1. The molecular weights reports are relative to standards of linear polyethyleneglycol (PEG) or poly(*N*,*N*-dimethylaminoethyl methacrylate) homopolymers quaternized with methyl iodide (quat. pDMAEMA).

Synthesis of lactobiono-O-(2-amidoethyl)-O'-(2-azidoethyl)-heptaethylene glycol **18**. Method 1. To a solution of lactobionic acid (419 mg, 1.17 mmol) in dry methanol (5 mL) were added O-(2-aminoethyl)-O'-(2-azidoethyl)-heptaethylene glycol (3) (1 eq., 1.17 mmol, 513 mg) and triethylamine (2 eq., 2.34 mmol, 320 µL). The mixture was stirred at 50°C overnight. The solvent was evaporated, the product rinsed with toluene and condensed. Without further purification, the product was dissolved in pyridine (10 mL) and an excess of acetic anhydride was added (4 mL, 42 mmol). The mixture was stirred for 15 min at 0°C and a small amount of 4-dimethylaminopyridine (DMAP) was added. The flask was then placed in an oil bath at 50°C and stirred for one hour. The solvent was removed under reduced pressure, the residue dissolved in ethyl acetate and washed successively with H2O, 2% citric acid, saturated sodium bicarbonate and brine. The aqueous phases were re-extracted twice with ethyl acetate. The organic phases were combined, dried on anhydrous magnesium sulfate and condensed. The crude mixture was purified by column chromatography on a silica column first using 1% methanol/dichloromethane, then 5% methanol/dichloromethane, leading to the amide 7 in 60% yield over the two steps. The alcohols were then deprotected using sodium methoxide (0.1 eq.) in anhydrous methanol. The mixture was stirred at room

temperature for one hour. Acid resin was used to remove sodium methoxide and the solvent was evaporated, leading to the clickable unit 10 in 36% yield over the three steps.

Following the previous protocol, lactobionic acid and the other PEG amino-azide compounds **13** and **14** were typically reacted together. The clickable units **19** and **20** were obtained in 36% and 45% yield respectively.

Method 2. Lactobionic acid was first partially converted to the corresponding lactobionolactone. This was achieved by dissolving lactobionic acid (25g, 70 mmol) and ca. 1 mL of trifluoroacetic acid in anhydrous methanol (150 mL) at 50°C, followed by vacuum distillation. The procedure was repeated three times until equilibrium was reached, and no further conversion could be observed. After solvent evaporation, the product was dried in the vacuum oven for 24 hours. In a second step, to a solution of this mixture (408 mg, 1.14 mmol) in dry methanol (5 mL) were added the PEG-7 amino-azide **12** (1 eq, 1.14 mmol, 500 mg) and triethylamine (2 eq, 2.28 mmol, 310 µL). The mixture was stirred at 50°C overnight and the solvent was evaporated. The mixture was passed through a short column of acid resin to remove the unreacted **12**, and **18** was obtained in 81% yield.

18. Rf = 0.69 (CH_3Cl_3/MeOH/H_2O 15/10/1). 〖[α]〗_D^19 +15.9 (c 1.02 in MeOH). 1H NMR (CD_3OD, δ, ppm): 4.49 (d, J 7.6, 1H), 4.36 (d, J 2.5, 1H), 4.23 (dd, J 2.5, 3.9, 1H), 3.93 (dd, J 4, 6.6, 1H), 3.85-3.90 (m, 1H), 3.75-3.84 (m, 4H), 3.62-3.76 (m, 31H), 3.53-3.61 (m, 4H), 3.35-3.52 (m, 6H). 13C NMR (CD_3OD, δ, ppm): 175.2, 105.8, 83.2, 77.2, 74.8, 73.9, 73.2, 72.8, 72.4, 71.6, 71.5 (8C), 71.3, 71.1, 70.6, 70.4, 63.8, 62.7, 51.8, 40.0. IR: 1649 (C=O), 2106 (N3). m/z (ESI+) 691 (M+H, 100%). m/z (HR-EI+) found: 691.3242; C26H51O17N4 691.3244.

19. Rf = 0.77 (CH_3Cl_3/MeOH/H_2O 15/10/1). 1H NMR (CD_3OD, δ, ppm): 4.48 (d, J 7.5, 1H), 4.36 (d, J 2.6, 1H), 4.21 (dd, J 2.6, 3.9, 1H), 3.93 (dd, J 3.9, 6.6, 1H), 3.85-3.90 (m, 1H),

3.74-3.84 (m, 5H), 3.61-3.73 (m, 38H), 3.53-3.60 (m, 4H), 3.36-3.52 (m, 6H). 13C NMR (CD_3OD, δ, ppm): 175.1, 105.7, 83.2, 77.2, 74.8, 73.9, 73.2, 72.8, 72.4, 71.6, 71.5 (12C), 71.3, 71.1, 70.5, 70.3, 63.8, 62.7, 51.8, 40.0. IR: 1646 (C=O), 2105 (N3). m/z (ESI+) 779 (M+H, 65%). m/z (HR-EI+) found: 779.3766; C30H59O19N4 779.3768.

20. Rf = 0.86 (CH_3Cl_3/MeOH/H_2O 15/10/1). 〖[α]〗 _D^21 +12.4 (c 1.02 in MeOH). 1H NMR (CD_3OD, δ, ppm): 4.48 (d, J 7.5, 1H), 4.36 (d, J 2.5, 1H), 4.22 (dd, J 2.5, 4, 1H), 3.93 (dd, J 3.9, 6.6, 1H), 3.87 (m, 1H), 3.74-3.84 (m, 4H), 3.61-3.72 (m, 47H), 3.53-3.60 (m, 4H), 3.34-3.52 (m, 6H). 13C NMR (CD_3OD, δ, ppm): 175.2, 105.8, 83.2, 77.2, 74.8, 73.9, 73.2, 72.8, 72.4, 71.6, 71.5 (16C), 71.3, 71.1, 70.6, 70.4, 63.8, 62.7, 51.8, 40.0. IR: 1647 (C=O), 2105 (N3). m/z (ESI+) 867 (M+H, 30%). m/z (HR-EI+) found: 867.4292; C34H67O21N4 867.4292.

Synthesis of macroRAFT p(DMAEMA): 1,1'-Azobiscyclohexanecarbonitrile (vazo 88, 5.65 mg, $2.31x10^{-5}$ mol), *bis*-RAFT agent 13 (20 eq, 428 mg, $4.63x10^{-4}$ mol), DMAEMA (3140 eq, 11.418 g, $7.26x10^{-2}$ mol) and DMF (42.36 mL, 40 g) were mixed together in a vial. After 30 min of stirring, the mixture was transferred in a 100 mL Schlenk flask and submitted to four freeze-pump-thaw cycles to remove oxygen. The flask was placed at 90°C for 17 hours; the reaction was then quenched by cooling and exposure to air. After 1H NMR determination of monomer conversion (see Scheme 4), the solvent was evaporated. The crude oil was diluted with dichloromethane (DCM) and the solution was precipitated by dropwise addition in heptane/diisopropyl ether 2/1. The solvent was decanted and the procedure repeated twice. The polymer was dissolved in DCM and the solvent evaporated overnight. 4.95 g of yellow solid foam were obtained. 1H NMR ($CDCl_3$, δ, ppm): 4.00-4.12 (bs, 2H, CH_2O), 2.51-2.63 (bs, 2H, CH_2N), 2.24-2.33 (bs, 6H, $N(CH_3)_2$), 1.71-2.06 (m, 2H, CH_2 backbone), 0.79-1.17

(m, 3H, CH_3 backbone). GPC in DMAc against PMMA standards: Mn = 23.5 kDa, PDI = 1.15.

Synthesis of TMS-protected PgMA: Silver chloride (1.46 g, $9.91x10^{-3}$ mol) was suspended in 145 mL of dry dichloromethane. Propargyl methacrylate (13 g, $1.05x10^{-1}$ mol) and DBU (20 mL, $1.34x10^{-2}$ mol) were added to the suspension, which became clear. The reaction mixture was heated to 40°C and trimethylsilane chloride (TMSCl, 19.8 mL, $1.49x10^{-1}$ mol) added dropwise via a syringe pump. The mixture was then stirred for 24 hours. The obtained dark red solution was diluted with 300 mL heptane and washed successively with water, 1% HCl, saturated NaHCO3 (200 mL each). The organic phase was dried on $MgSO_4$, filtered and concentrated under reduced pressure. The crude product was purified by silica column chromatography in a heptane/diethyl ether 25/1 mixture to afford PgMA in 74% yield. 1H NMR ($CDCl_3$, δ, ppm): 6.17 (m, 1H, C=CH), 5.61 (m, 1H, C=CH'), 4.76 (s, 2H, CH_2), 1.96 (m, 3H, CH_3), 0.18 (s, 9H, TMS). 13C NMR ($CDCl_3$, δ, ppm): 166.8 (C=O), 135.9 (CH_2=C), 126.5 (CH_2=C), 99.4 (CH_2-C≡C), 92.1 (C≡C-TMS), 53.5 (CH_2O), 18.4 (CH3), -0.1 ($Si(CH_3)_3$). IR: 2200 (weak, C≡C stretch), 1723 (strong, C=O stretch), 1639 (medium, C=C stretch).

*Synthesis of the ABA triblock **10**:* AIBN (1.03 mg, 6.2x10-6 mol), pDMAEMA (590.2 mg, 2.51x10-5 mol), TMS-PgMA (54.8 mg, 2.79x10-4 mol) and HPMA (323.79 mg, 2.26x10-3 mol) were mixed together in a vial with DMAc (total monomer concentration 0.7 mol/L). The ratio HPMA to TMS-PgMA was 9/1 and the total molar ratio of monomer to pDMAEMA (macro RAFT agent) to initiator was 100/1/0.25. The mixture was transferred in a Schlenck flask, submitted to four freeze-pump-thaw cycles and placed in a 60 °C oil bath. After 24 hours, the reaction was quenched by cooling and exposure to air and NMR analysis was used to determine monomer conversions: PgMA conversion = 80% (8 units per chain) and HPMA conversion = 47% (42 units per chain). M(th) = 25.7 kDa. The solvent was evaporated, the

polymer was dissolved in methanol and precipitated in a mixture of diethyl ether and pentane 1/1.5 4 times. 1H NMR (CD3OD, δ, ppm): 7.35-7.60 (bs, 1H, NH (HPMA) partially exchanged), 4.51-4.73 (bs, 2H, CH_2O (PgMA)), 4.03-4.21 (bs, 2H, CH_2O (DMAEMA)), 3.79-3.96 bs, 1H, CH (HPMA)), 2.89-3.26 (m, 2H, CH_2 (HPMA)), 2.60-2.74 (bs, 2H, CH_2N (DMAEMA)), 2.27-2.44 (m, 6H, $N(CH_2)_3$ (DMAEMA)), 0.80-2.23 (m, CH_2 and CH_3 backbone + CH_3 (HPMA)), 0.15-0.27 (bs, 9H, TMS (PgMA)). PgMA/HPMA/DMAEMA = 1/3.8/9.6, M(NMR) = 26.6 kDa. GPC in DMAc against PMMA standards: Mn = 36.4 kDa, PDI = 1.18.

For the second batch, all the quantities were multiplied by 5 and the same procedure was followed. NMR analysis was used to determine monomer conversions: PgMA conversion = 80% (8 units per chain) and HPMA conversion = 33% (30 units per chain). M(th) = 24 kDa. The solvent was evaporated and the polymer was precipitated 4 times in a cold diethyl ether/pentane mixture 1/1.5, paying particular attention to the dilutions in minimal amounts of methanol. The NMR spectrum of the precipitated polymer showed the same peaks as the previous batch. PgMA/HPMA/DMAEMA = 1/4.7/15.7, M(NMR) = 24.3 kDa. GPC in DMAc against PMMA standards: Mn = 33 kDa, PDI = 1.33.

*Deprotection to ABA triblock **11**:* 225 mg of the ABA triblock 16 (M = 26.4 kDa, DP(PgMA) = 10, $8.52x10^{-5}$ mol TMS groups) were dissolved in 15 mL of THF. One drop of acetic acid was added, the mixture was bubbled with nitrogen for 10 min and cooled down to -20 °C. TBAF in solution in THF (0.2 M, 0.5 mL, 1.1 eq., $9.4x10^{-5}$ mol) was slowly added via syringe. The mixture was stirred at this temperature for 30 min, then warmed to ambient temperature and stirred for 3 more hours. The reaction solution was passed through a short silica pad in order to remove the excess of TBAF and the pad was subsequently washed with additional THF. The resulting solution was then concentrated under reduced pressure. The crude polymer was dissolved in methanol and precipitated in a cold diethyl ether/pentane

1/1.5 mixture. 1H NMR (CD_3OD, δ, ppm): 7.35-7.60 (bs, 1H, NH (HPMA) partially exchanged), 4.51-4.73 (bs, 2H, CH_2O (PgMA)), 4.03-4.21 (bs, 2H, CH_2O (DMAEMA)), 3.79-3.96 bs, 1H, CH (HPMA)), 2.89-3.26 (m, 2H, CH_2 (HPMA)), 2.60-2.74 (bs, 2H, CH_2N (DMAEMA)), 2.27-2.44 (m, 6H, $N(CH_2)_3$ (DMAEMA)), 0.80-2.23 (m, CH_2 and CH_3 backbone + CH_3 (HPMA)). GPC in DMAc against PMMA standards: Mn = 36 kDa, PDI = 1.24.

For the second batch of ABA triblock, the same molar ratios and procedure were used for the deprotection of 2.1 g of the ABA triblock (M = 24.3 kDa, DP(PgMA) = 8, 6.91x10-4 mol TMS groups). The NMR spectrum of the precipitated polymer (20) showed the same peaks as the previous batch. GPC in DMAc against PMMA standards: Mn = 39.8 kDa, PDI = 1.25.

*Grafting of the targeting units **18**, **19**, **20**, **30** and **31** on polymer **11** by click reaction:*[34] 100 mg of the deprotected ABA triblock **11** (M = 23.7 kDa, DP(PgMA) = 8, $1.6x10^{-5}$ mol alkyne groups), the clickable unit (1.5 eq., $5.04x10^{-5}$ mol, 34.8 mg , 39.2 mg, 43.7 mg, 38.5 mg and 42.9 mg for **18**, **19**, **20**, **29** and **30**, respectively) and PMDETA (1.9 μL, 0.3 eq, 9.24x10-6 mol) were solubilized in 4 mL DMF. The solution was bubbled with nitrogen for 15 min and copper bromide was added (1.3 mg, 0.3 eq., $9.24x10^{-6}$ mol). The solution was bubbled 10 min more and stirred at room temperature for 24 hours. Quadrasil resin (ca. 100 mg) was added and the mixture was gently stirred for 2 days, filtered and condensed under reduced pressure at 50°C. The crude products **32-36** were purified by size exclusion chromatography in a LH-20 column in DMF.

32. 1H NMR (CD_3OD, δ, ppm): 8.10-8.20 (bs, 1H (PgMA), triazole), 4.61-4.70 (bs, 2H (PgMA), CH_2O), 4.02-4.20 (bs, 2H (DMAEMA), CH_2O), 3.77-4.00 (m, 1H (HPMA), CH + 7H (**18**)), 3.66-3.73 (m, 34H (**18**)), 2.92-3.24 (m, 2H (HPMA), CH_2), 2.60-2.73 (bs, 2H (DMAEMA), CH_2N), 2.28-2.41 (m, 6H (DMAEMA), $N(CH_2)_3$), 0.79-2.21 (m, 5H (PgMA) +

8H (HPMA) + 5H (DMAEMA), CH_2 and CH_3 backbone + CH_3 (HPMA)). GPC in DMAc against PMMA standards: Mn = 55.3 kDa, PDI = 2.05.

33. 1H NMR (CD_3OD, δ, ppm): 8.08-8.24 (bs, 1H (PgMA), triazole), 4.61-4.68 (bs, 2H (PgMA), CH_2O), 4.48-4.54 (bs, 1H (**19**)), 4.36-4.39 (bs, 1H (**19**)), 4.22-4.26 (bs, 1H (**19**)), 4.03-4.19 (bs, 2H (DMAEMA), CH_2O), 3.77-3.99 (m, 1H (HPMA), CH + 7H (**19**)), 3.56-3.70 (m, 48H (**19**)), 2.93-3.24 (m, 2H (HPMA), CH_2), 2.60-2.73 (bs, 2H (DMAEMA), CH_2N), 2.28-2.41 (m, 6H (DMAEMA), $N(CH_2)_3$), 0.73-2.20 (m, 5H (PgMA) + 8H (HPMA) + 5H (DMAEMA), CH_2 and CH_3 backbone + CH_3 (HPMA)). GPC in DMAc against PMMA standards: Mn = 57.5 kDa, PDI = 1.49.

34. 1H NMR (CD_3OD, δ, ppm): 8.07-8.25 (bs, 1H (PgMA), triazole), 4.61-4.68 (bs, 2H (PgMA), CH_2O), 4.49-4.54 (bs, 1H (20)), 4.37-4.39 (bs, 1H (20)), 4.22-4.26 (bs, 1H (20)), 4.05-4.17 (bs, 2H (DMAEMA), CH2O), 3.78-3.98 (m, 1H (HPMA), CH + 6H (20)), 3.56-3.69 (m, 57H (20)), 2.92-3.25 (m, 2H (HPMA), CH2), 2.60-2.73 (bs, 2H (DMAEMA), CH_2N), 2.28-2.41 (m, 6H (DMAEMA), N(CH2)3), 0.80-2.20 (m, 5H (PgMA) + 8H (HPMA) + 5H (DMAEMA), CH2 and CH3 backbone + CH3 (HPMA)). GPC in DMAc against PMMA standards: Mn = 48.5 kDa, PDI = 1.71.

35. 1H NMR (CD_3OD, δ, ppm): 8.08-8.25 (bs, 1H (PgMA), triazole), 5.02-5.21 (bs, 1H, (**30**)), 4.74-5.00 (bs, 2H (PgMA), CH_2O), 4.56-4.71 (bs, 1H (**30**)), 4.30-4.46 (bdd, 1H (**30**)), 3.97-4.20 (bs, 2H (DMAEMA), CH_2O), 3.79-3.96 (m, 1H (HPMA), CH + 7H (**30**)), 3.47-3.72 (m, 57H (**30**)), 2.89-3.44 (m, 2H (HPMA), CH_2), 2.54-2.72 (bs, 2H (DMAEMA), CH_2N), 2.23-2.38 (m, 6H (DMAEMA), $N(CH_2)_3$), 0.74-2.10 (m, 5H (PgMA) + 8H (HPMA) + 5H (DMAEMA), CH_2 and CH_3 backbone + CH_3 (HPMA)). GPC in DMAc against PMMA standards: Mn = 41.4 kDa, PDI = 1.41.

36. 1H NMR (CD_3OD, δ, ppm): 8.07-8.20 (bs, 1H (PgMA), triazole), 5.01-5.24 (bs, 1H, (**31**)), 4.76-4.96 (bs, 2H (PgMA), CH_2O), 4.55-4.69 (bs, 1H (**31**)), 4.29-4.46 (bdd, 1H (**31**)), 3.96-4.20 (bs, 2H (DMAEMA), CH_2O), 3.77-3.95 (m, 1H (HPMA), CH + 7H (**31**)), 3.47-3.76 (m, 57H (**31**)), 2.87-3.42 (m, 2H (HPMA), CH_2), 2.53-2.73 (bs, 2H (DMAEMA), CH_2N), 2.19-2.40 (m, 6H (DMAEMA), $N(CH_2)_3$), 0.72-2.11 (m, 5H (PgMA) + 8H (HPMA) + 5H (DMAEMA), CH_2 and CH_3 backbone + CH_3 (HPMA)). GPC in DMAc against PMMA standards: Mn = 41.4 kDa, PDI = 1.50.

Cells:

Chinese Hamster Ovary cells constitutively expressing Green Fluorescent protein (CHO-GFP) (kindly received from K. Wark; CSIRO CMHT Australia) were grown in MEMα modification supplemented with 10% foetal bovine serum, 10 mM Hepes, 0.01% penicillin and 0.01% streptomycin at 37 ºC with 5% CO_2 and subcultured twice weekly. Human adenocarcinomic human alveolar basal epithelial cells (A549) and human hepatocarcinoma (huh7) cells were grown in DMEM supplemented with 10% foetal bovine serum, 10 mM Hepes, 2 mM glutamine, 0.01% penicillin and 0.01% streptomycin at 37 ºC with 5% CO_2 and subcultured twice weekly.

Toxicity Assay:

CHO-GFP, A549 and Huh7 cells were seeded at $2x10^4$ cells in 96-well tissue culture plates in triplicate and grown overnight at 37 ºC with 5% CO_2.

The serially diluted polymer materials or polymer/diRNA complexes were added to 3 wells in the 96 well culture plates for each sample and incubated for 72 h at 37 ºC in 200 µl standard media. Toxicity was measured using the Alamar Blue reagent (Invitrogen USA) according to manufacturer's instructions. Briefly, media was removed, cells were washed

with PBS and replaced with 100 µl of standard media containing 10% Alamar Blue reagent, cells were then incubated for 4 h at 37 ºC with 5% CO_2. The assay was read on an EL808 Absorbance microplate reader (BIOTEK, USA) at 540 nm and 620 nm. Cell viability was determined by subtracting the 620 nm measurement from the 540 nm measurement. Obtained data was analysed in Microsoft Excel. Results are presented as a percentage of untreated cells and the presented data are representative of three separate experiments in triplicate.

siRNA:

The anti-GFP and negative control siRNAs were obtained from QIAGEN (USA).

The anti-GFP siRNA sequence is sense 5' gcaagcugacccugaaguucau 3' and antisense 5'gaacuucagggucagcuugccg 3'. [6 FAM] labelled si22 was purchased from Sigma Aldrich (USA) with the FAM label on the sense strand.

The non-silencing control is the same sequence as the siRNA as a DNA duplex. This will not be recognised by RISC, therefore should nit silence GFP.

The siDeath siRNA mix was obtained from QIAGEN.

The anti-COPA siRNA sense sequences are

siCOPA-1 ACUCAGAUCUGGUGUAAUA[dT][dT]

siCOPA-2 GCAAUAUGCUACACUAUGU[dT][dT]

siCOPA-3 GAUCAGACCAUCCGAGUGU[dT][dT]

siCOPA-4 GAGUUGAUCCUCAGCAAUU[dT][dT]

Formation of polymer/siRNA complexes:

Molar ratios of polymer to 50 pmole siRNA or siDNA were calculated. Complexes were formed by the addition of OPTIMEM media (Invitrogen, USA) to eppendorf tubes. The required amount of polymer resuspended in water was added to the tubes and the mixture vortexed. 50nM of si22 or di22 was then added to the tubes and the sample vortexed. Complexation was allowed to continue for 1 h or overnight at room temperature.

Agarose gel:

Samples containing 50 pmole of siRNA were electrophoresed on a 2% agarose gel in TBE at 100V for 40 min. siRNA was visualised by gel red (Jomar Bioscience) on a UV transilluminator with camera, the image was recorded by the GeneSnap program (Syngene, USA).

Silencing Assay:

CHO-GFP cells were seeded at $1x10^4$ cells in 96-well tissue culture plates in triplicate and grown overnight at 37 ºC with 5% CO_2. For positive and negative controls siRNAs were transfected into cells using Lipofectamine 2000 (Invitrogen, USA) as per manufacturer's instructions. Briefly, 50 picomole of the relevant siRNA were mixed with 1 µl of Lipofectamine 2000 both diluted in 50 µl OPTI-MEM (Invitrogen, USA) and incubated at room temperature for 20 mins. The siNA: lipofectamine mix was added to cells and incubated for 4 h. Cell media was replaced and incubated for 72 h.

For polymer/siRNA complexes prepared, cell media was removed and replaced with 200 µl OPTI-MEM. The siRNA: polymer complexes in a volume of 10µl was added to 3 wells of cells per sample and incubated for 5 h. Cell media was replaced and cells incubated for a further 72 h.

Cells were washed twice with PBS, and read on a Fluoroskan Ascent FL (Thermo Scientific, USA) and EGFP silencing was analysed as a percentage of the siDNA or polymer/siDNA complexes mean EGFP (ex 488nm em 516nm) fluorescence.

For A549 and Huh7 cells; Cell death was determined by the Alamar Blue reagent (Invitrogen USA) according to manufacturer's instructions. Briefly, media was removed, cells were washed with PBS and replaced with 100 µl of standard media containing 10% Alamar Blue reagent, cells were then incubated for 4 h at 37 ºC with 5% CO_2. The assay was read on an EL808 Absorbance microplate reader (BIOTEK, USA) at 540 nm and 620 nm. Cell viability was determined by subtracting the 620 nm measurement from the 540 nm measurement. Obtained data was analysed in Microsoft Excel. Results are presented as a percentage of di22 control treated cells and the presented data are representative of three separate experiments in triplicate.

Uptake of [6'FAM] si22

Polymer/si22-FAM complexes (50 pmol) were assembled as described above using the [6FAM] labelled si22.

Flow cytometry; CHO-WT cells were seeded at 1x105 cells in 96-well tissue culture plates in triplicate (Nunc, USA) and grown overnight at 37ºC with 5% CO2. For positive controls [6FAM] labelled si22 was transfected into cells using Lipofectamine 2000 as described above. Polymer and labelled siRNA complexes were produced as described above and added to the cells for 5 or 24 hrs. Cells were washed with PBS, trypsinised and washed twice with FACS wash (PBS with 1% FBS). Cells were subjected to flow cytometry and the FITC fluorescence at emission of 516 nm was analysed in Microsoft Excel based on the uptake index which is the percentage of cell transfected multiplied by the mean fluorescence of the transfected cell population. Results are presented relative to [6FAM] labelled si22 alone

treated cells and the presented data are representative of three separate experiments in triplicate.

RESULTS AND DISCUSSION

Synthesis of alkyne-bearing polymers

The polymer synthesis started with the synthesis of a biodegradable disulfide-containing *bis*-RAFT agent **5**, which was derived through standard coupling of the trithiocarbonate **3** and alcohol **4** (Scheme 1). Our previous studies have demonstrated the optimal central pDMAEMA block of the polymer is 110 units to be an effective siRNA carrier, with low toxicity, which was synthesised employing standard RAFT protocols with DMAEMA **6 [14]**. Thus, the resulting pDMAEMA macro RAFT agent **7** was purified by precipitation and characterized by ^{1}H NMR and gel permeation chromatography (GPC). The calculated Mn of the pDMAEMA was 18.2 kDa (based on the NMR determination of the monomer conversion (70%)), and the molecular weight determined by GPC (23.4 kDa). As expected, the polydispersity of this polymer was narrow, 1.15 (Table 1).

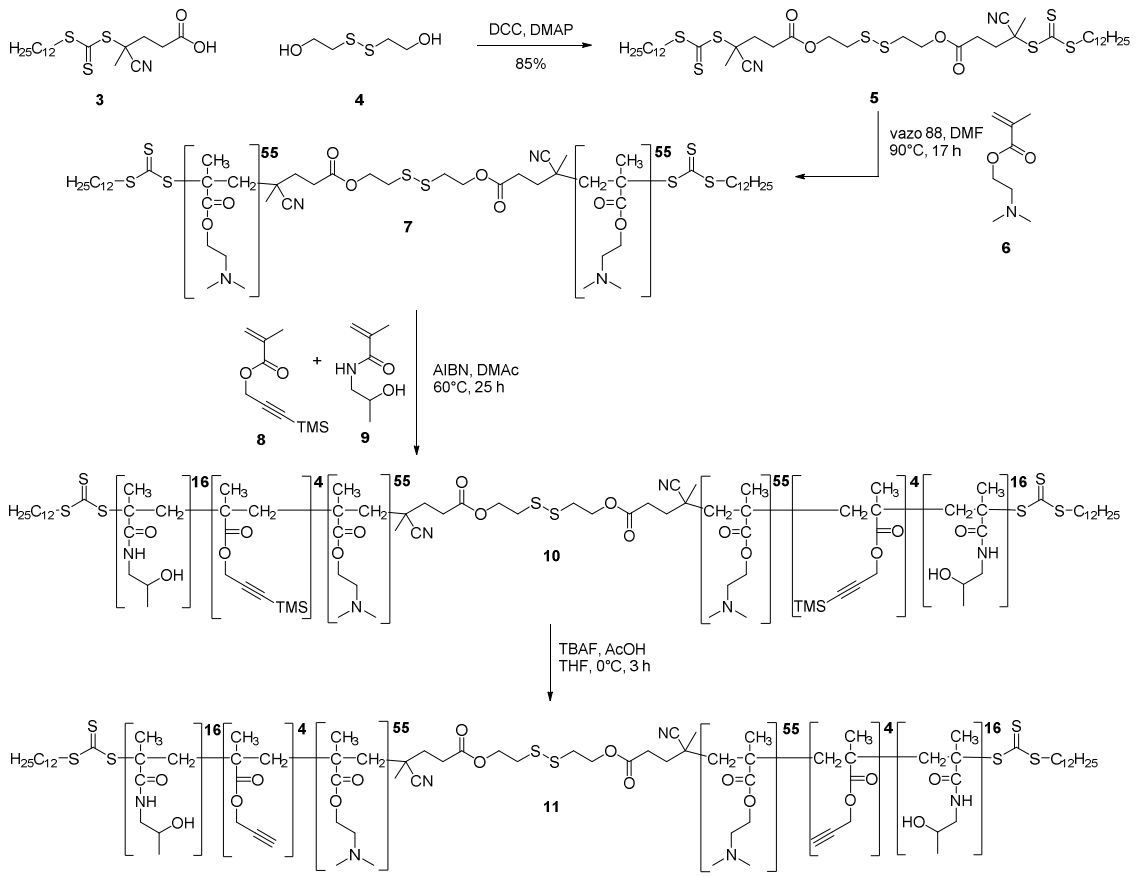

Scheme 1: Synthesis of alkyne-bearing RAFT ABA-triblock copolymers

To obtain a discrete distribution of alkyne functionality randomly dispersed in the outer blocks of the pDMAEMA **7**, the hydrophilic monomer HPMA **9** was copolymerized with trimethylsilyl-propargyl methacrylate (TMS-PgMA) **8**. The TMS protecting group is the established method to prevent the alkyne groups participating in radical reactions during the polymerisation process[31]. Indeed, our early attempts with PgMA gave polymers with much broader polydispersity. This may be attributed to the involvement of the alkyne groups in the radical addition process, probably leading to cross-linking and branching phenomena.[35] The TMS protected PgMA **8** was conveniently synthesized by treating PgMA with TMS-Cl in the presence of AgCl.[36] Thus, TMS-PgMA **8** was copolymerized with HPMA **9** in DMAc using standard RAFT protocols to give the ABA-triblock copolymer **10**. ^{1}H NMR analysis showed

that the obtained ABA-triblock copolymer **10** contained 33 HPMA units and 7 PgMA units per polymer chain (for a calculated molecular weight of 24.3 kDa). The GPC against polymethylmethacrylate (PMMA) standards found a polydispersity of 1.33 and molecular weight 33 kDa. The ABA-triblock copolymer **10** was then easily deprotected using tetrabutylammonium fluoride (TBAF) in THF. The NMR analysis showed complete disappearance of the TMS peak and GPC analysis confirmed a slight decrease in MW from 36.4 kDa to 35.9 kDa.

Synthesis of azide-bearing ASGPR targeting groups

The synthesis of the galactose targeting group took advantage of commercially available lactobionic acid which is ideally configured, in that it bears a β-galactose group and a convenient spacer between the targeting group and the PEG linker, allowing conformational flexibility during ligand binding. Lactobionic acid was condensed directly with three different amines (Compounds **12-14**) containing azide end groups and polyethylene glycol chains (PEG) with increasing EG repeats from 5 to 9 units. The reaction presumably proceeded through the *in situ* formation of the lactone **21**, and after acetate protection, delivers the amides **15-17** in 50 to 60% yield over the two steps. Acetate protection was used to aid with purification of the products. With pure compounds in hand, the acetates **15**, **16**, and **17** were deprotected, leading to clickable targeting agents **18**, **19** and **20** in 35 to 45% yield over the three steps, respectively (Scheme 2).

An alternate approach was also investigated, which consisted of converting the lactobionic acid to lactobionolactone **21** prior to reaction with the PEG amine compounds **12**, **13** and **14**[37]. Despite incomplete conversion of lactobionic acid to the lactone **21**, this route led to amides **18**, **19** and **20** in excellent yields of 81% yield. Key to this conversion was the removal of any excess amine **12**, **13** or **14** with Amberlyst 15 resin, which delivered material

comparable to that synthesised through the protection method and required no further purification (Scheme 2).

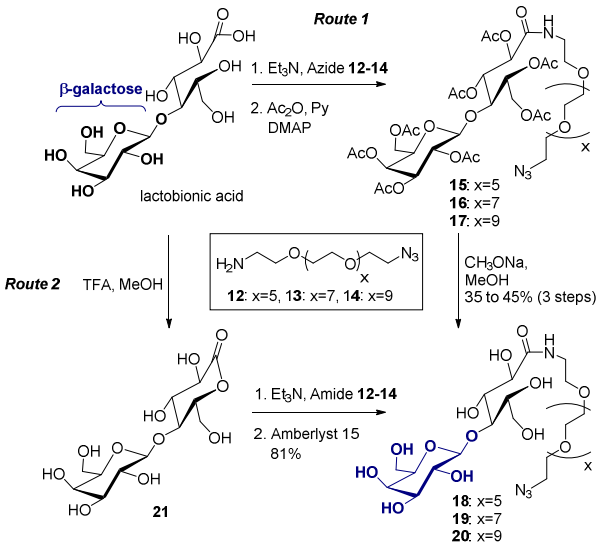

Scheme 2: The synthesis of azide-bearing galactose ASPGR targeting groups.

Synthesis of the glucose controls was performed via a similar protocol, employing commercially available cellobiose **22**, to mimic the galactose linker strategy. An initial approach was to oxidise cellobiose into cellobionolactone for the facile introduction of the azide-bearing PEG linker (Scheme 3) however, the lactone appeared unreactive towards amide formation under a range of conditions.[38] A second option involved oxidation and amide formation in one step, which was attempted with a model amine, ethylamine.[39] Upon acetyl protection of the resultant amide, only a 5% yield of the product was gained. It was therefore deemed necessary to attach the azido-PEG groups through a glycosyl link by initially activating the anomeric alcohol and displacing it with a hydroxyl terminated azide-bearing PEG linker. For this approach, cellobiose was fully protected as acetyl cellobiose **23** before deprotection of the anomeric hydroxyl using hydrazine in DMF at 50 °C. The anomeric alcohol **24** was converted into the trichloroacetimidate **25** for the addition of PEG-7 and PEG-9 linkers, **26** and **27**, respectively, employing TMSOTf and molecular sieves. The

resultant 1:1 α/β anomeric mixtures **28** and **29** were then deprotected with NaOMe in methanol to provide the glucose-containing PEG-7 and PEG-9 glycosides **30** and **31**, respectively (Scheme 3). Whilst it was decided to carry the 1:1 α/β anomeric mixture forward without separation, it is worthy to note that the terminal glucose residue (like the galactose analogue) exists exclusively as its β-anomer.

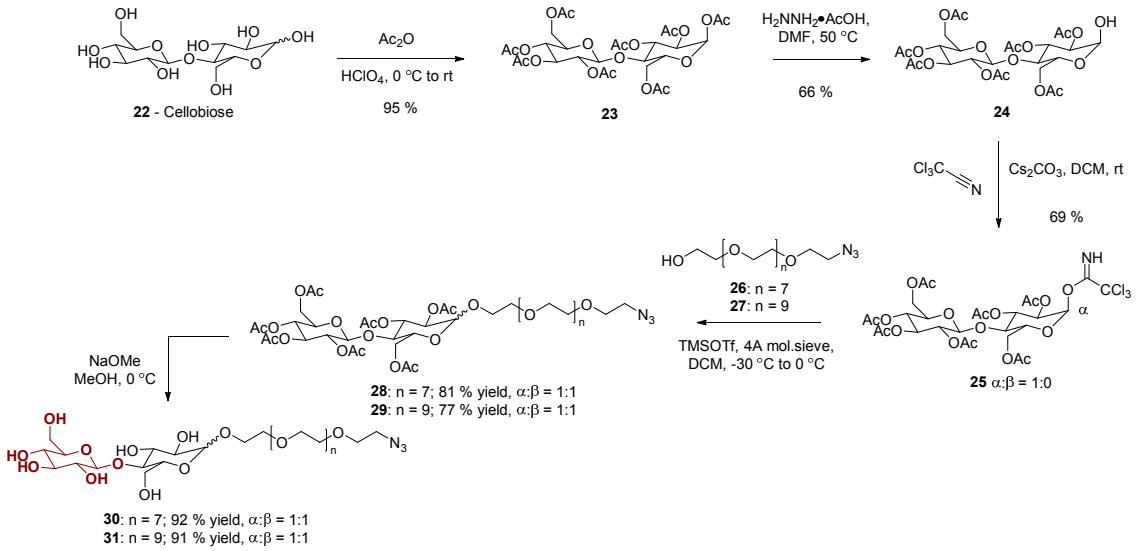

Scheme 3: Synthesis of azide-bearing glucose control moieties

Grafting of the ASGPR targeting and glucose control units.

The targeting units **18**, **19**, **20**, **30** and **31** were grafted in parallel onto the polymer **11**, in the presence of copper bromide as the catalyst and *N*,*N*,*N'*,*N*",*N*"-pentamethyldiethylenetriamine (PMDETA) as the ligand,[33] leading to the polymers **32**, **33**, **34**, **35** and **36**. GPC analysis showed that the polymeric products contained azide starting material. Early attempts to purify by dialysis were unsuccessful (data not shown). Purification by precipitation was similarly unsuccessful because of the similarly in solubility of the azides (**18-20, 30, 31)** and the resulting polymers. However, purification of the obtained polymers by size exclusion chromatography (Sephadex LH-20) allowed completed removal of the excess clickable units

and also reduced the levels of copper in the final material from 45-65 ppm to 9-13 ppm, below the biologically acceptable level for copper concentrations in a final product (15 ppm)[40].

Polymer	Block B (pDMAEMA): molar mass (Mn in kDa)/dispersity	Tri-block ABA: GPC molar mass (Mn in kDa)/dispersity[a]	Tri-block ABA: NMR molar mass (Mn in kDa)	Tri-block ABA: Theoretical grafted molar mass (Mn in kDa)
7	23.4/1.15	-	18.2[b]	-
10	-	33/1.33	24.3	-
11	-	36/1.24	-	-
32	-	55.3/2.05	-	41.5
33	-	57.5/1.49	-	42.2
34	-	48.5/1.71	-	42.9
35	-	41.4/1.41	-	42.2
36	-	41.4/1.50	-	42.9

[a] The GPC data relative to PMMA standard. [b] NMR determination of Mn based on monomer conversion.

Table 1: The number average molecule weight, dispersity, and composition of the block copolymers prepared from TMS-PgMA, HPMA, and DMAEMA using RAFT polymerization.

The formation of the grafted ABA-triblock copolymers was assessed both by ^{1}H NMR analysis, which showed the appearance of the triazole peak at 8.1 ppm, and by GPC, which showed a molecular weight increase from 36 kDa to 55.3, 57.5, and 48.5 kDa (lactobiose linkers) and 41.4 kDa (cellobiose linkers), respectively (Table 1). This increase in molecular

weight is significantly higher than the theoretical expected value resulting from grafting of 5.5, 6.2, 6.9, 6.2 and 6.9 kDa (i.e., 8 x **18**, **19**, **20**, **30** and **31**) onto polymer **11**, respectively. However, given the molar mass values for the precursor PgMA-HPMA-DMAEMA ABA triblock copolymer **11** and the grafted polymers **18**, **19**, **20**, **30** and **31** were determined relative to polymethylmethacrylate (PPMA) standards, this discrepancy may result from the significantly different physical properties of the grafted material leading to altered GPC behaviour compared to that of the parent material **11**.

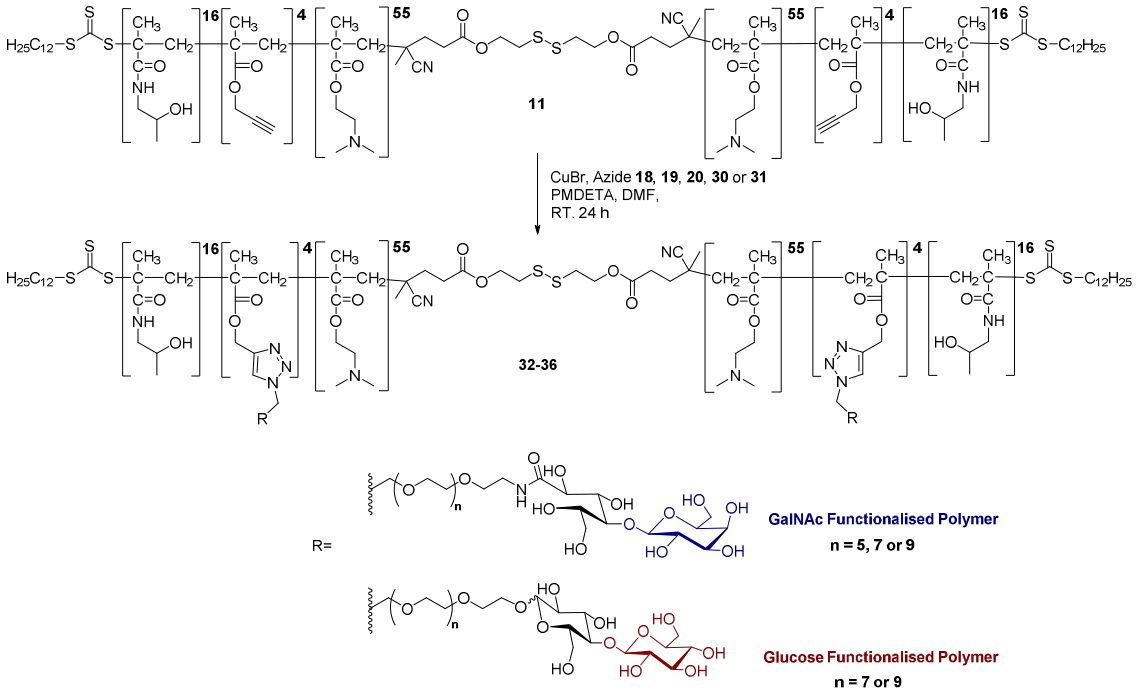

Scheme 4: Grafting of ASGPR targeting groups onto the polymer backbone using CuAAC 'click' chemistry.

In our previous work, the ABA triblock copolymer has been evaluated biologically in its quaternized state following treatment of the neutral parent polymer with methyl iodide. To understand the necessity of quaternization for siRNA carrying efficacy, polymers **32-36** were submitted to biological assay in both their unquaternized and quaternized forms. Quaternization of these polymers using methyl iodide in DMF provided polymers bearing a

permanent cationic charge. Those polymers not quaternized are denoted as "Not Q" in the following section (Scheme 5).

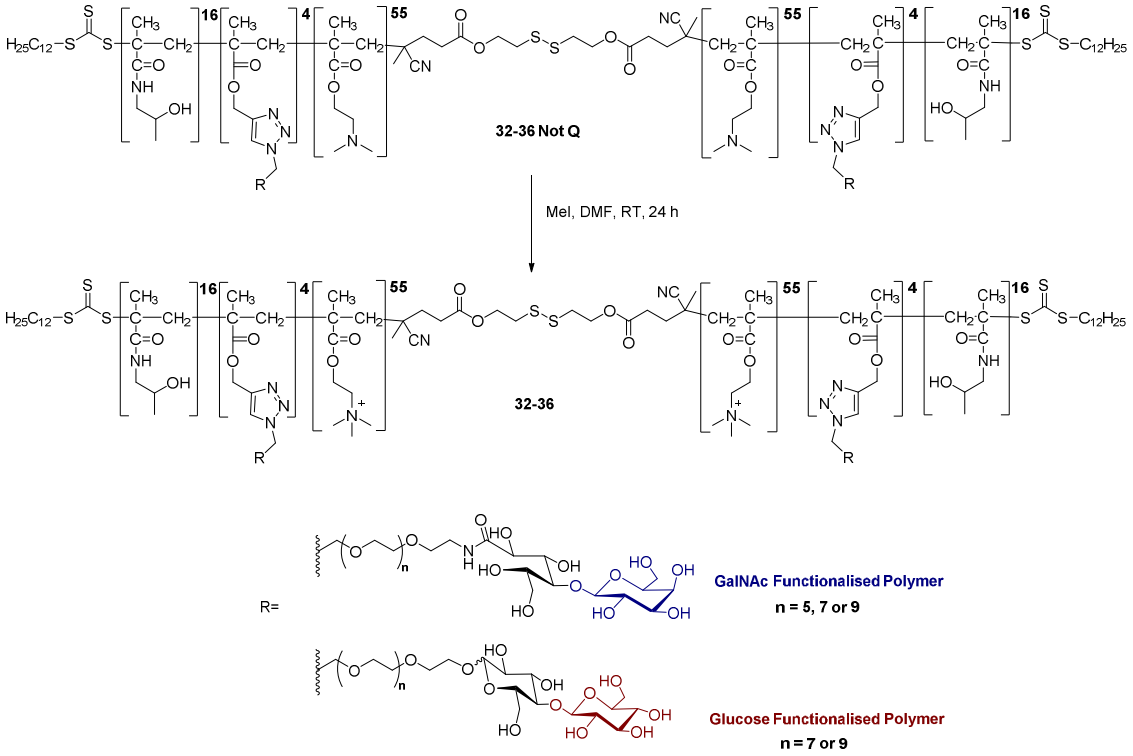

Scheme 5: Quaternisation of polymers using methyl iodide.

BIOLOGICAL RESULTS

siRNA Binding Assay:

To understand the binding ability of the quaternized and unquaternized glycosylated polymers, polyplexes prepared with different siRNAs, and at different N:P ratios, were evaluated by agarose gel electrophoresis (Fig. 5). siRNA binding ability was determined by

comparison to a control well of naked siRNA, showing siRNA migration on the gel when not in the polyplex.

Results for binding with si22 (anti-Green Fluorescent Protein (GFP)) (Fig. 5A) showed that an N:P of 10 provided the best binding, with little to no unbound si22. An N:P of 5 might be preferable, however, to ensure the siRNA may be released from the polyplex and is not bound too tightly by electrostatic interactions, preventing release. From transfection results with our previous non-functionalised ABA triblock we postulated that a too tightly bound polyplex was to blame for low transfection (unpublished results) – this is a significant challenge for delivery vectors to maintain a careful balance between a stable polyplex and cargo release for efficient transfection[41]. As expected the unquaternized polyplexes showed release of si22, but not to the extent we had predicted (unpublished hypothesis). For siDeath, which consists a mix of 4 siRNAs targeting essential cell genes (Fig. 5B), N:P of 5 and above showed little unbound siRNA, with the glucose functionalised polymers showing tighter binding than the galactose functionalised polymers. Again, unquaternized polymers displayed good binding with siDeath, indicating that a permanent cationic charge may not be necessary for polyplex formation. Interestingly, a second apoptosis inducing siRNA targeting the Coatomer Protein Complex Subunit Alpha, siCOPA (Fig. 5C) is not so tightly bound to the glycosylated ABA polymer, even at N:P 10.

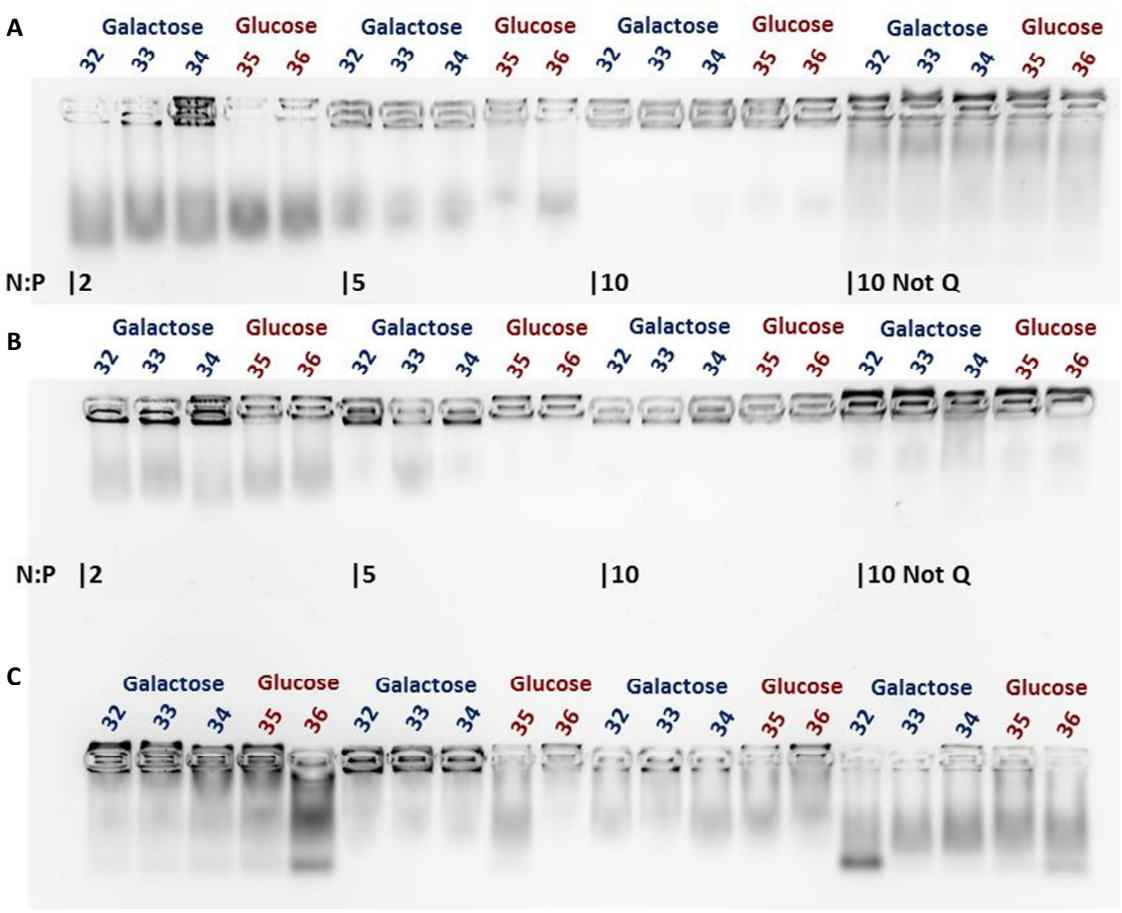

Figure 5: Gel electrophoresis results indicating qualitative binding efficiency of the functionalised polymers, tested at a polymer to siRNA molar ratios in the range of 2-10 at a fixed amount of siRNA (50 pmol). Samples were electrophoresed at 100 V for 40 min on a 2% agarose gel and visualised by gel red (Jomar Bioscience) on a UV transilluminator with camera. The image was recorded by GeneSnap program (Syngene, USA). **(A)** = si22 (GFP); **(B)** = siDeath; **(C)** = siCOPA.

Toxicity and Gene Silencing:

Cell viability in the presence of the polymers was evaluated in Chinese Hamster Ovary cells constitutively expressing GFP (CHO-GFP) without siRNA association **(**Fig. 6A, dotted line**)**. Compared to a positive control of Lipofectamine (a commercially available delivery vector), polymers showed low toxicity, with cell viabilities around or above 80%. Polymers **32-36**

were assessed in CHO-GFP cell lines, to evaluate silencing of fluorescence by si22-polymer complexes (Fig. 6A). Lipofectamine, a commercially available delivery vector, was used as a positive control. Lipofectamine shows low toxicity and a gene silencing efficiency of 60% when complexed with siRNA. All polymers show around 40-50% GFP knockdown at N:P 10, in both quaternized and unquaternized forms. At N:P's of 2 and 4, little to no gene silencing is observed. This suggests that either the si22 is too tightly bound to the polymer, the galactose is not displayed for efficient interaction with the ASGPR or that the particle size, elasticity and zeta potential at the lower ratios is inefficient at entering the cell to deliver the si22 cargo. Future physicochemical analysis of these particles is required, as this analysis has been shown to be very important in nanoparticle delivery.[42]

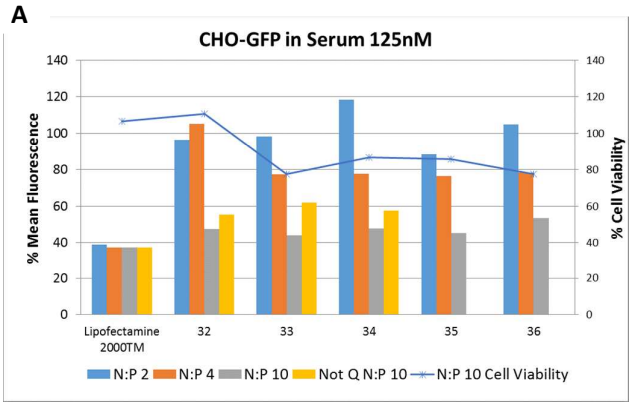

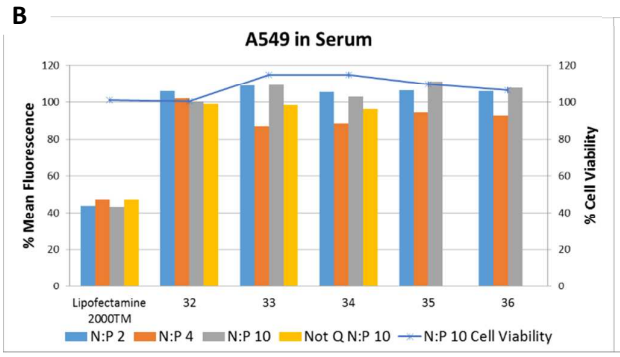

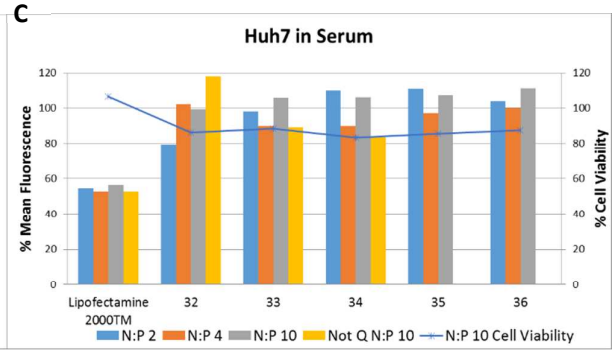

Figure 6: Toxicity (% cell viability, dots) and silencing assays (% GFP fluorescence, bars) for polymers **32-36** at N:P's of 2 (orange); 4 (yellow) and 10 (green). Unquaternized polymers at N:P 10 were also included (red). **(A)** GFP knockdown in CHO-GFP cells; **(B)** GFP knockdown in A549 cells; **(C)** GFP knockdown in Huh7 cells. Samples were added to cells for 72 h, after which the cells were washed with FACS buffer, trypsinised and analysed on a BD LSRII flow cytometer for GFP fluorescence. Results are presented as % GFP knockdown compared to the equivalent Lipofectamine 2000 transfected si22 control.

The polyplexes were then analysed for their transfection efficiency in A549 (human lung carcinoma) cell lines (Fig. 6B). Since these cells lines do not possess ASGP receptors, it would be expected that uptake of polymers would occur through other endocytosis mechanisms, thus there should be little difference between the galactose- and glucose-functionalised polymers. This was indeed the case, however, both polymer series show little to no knockdown, and therefore no substantial conclusions can be drawn.

The Huh7 cell line is a hepatocyte-derived cell line **(**Fig. 6C**)**, known to be decorated with ASGP receptors[43], and therefore should show higher uptake for the galactose-functionalised polymers due to clathrin-mediated endocytosis. Again, there is little difference between the glucose control and the galactose-bearing polymers. The PEG-5 galactose linked polymer **32** does show 20% GFP knockdown at an N:P of 2, but this is a very inefficient delivery vector compared to Lipofectamine (50% GFP knockdown).We had postulated that a longer linker

length (PEG-9) might provide greater degrees of freedom for the targeting functionality, and therefore increased ASGP receptor recognition and binding, and uptake. Surprisingly, PEG-linker length did not provide any differentiation in GFP knockdown efficiency. Interestingly in A549 cells, uptake of galactose containing complexes was improved with a liker length of 7 and 9, whilst in Huh7 cells the shorter linker allowed greater uptake of the complexes. This corresponds with the silencing observed in Huh7 cells with this polymer.

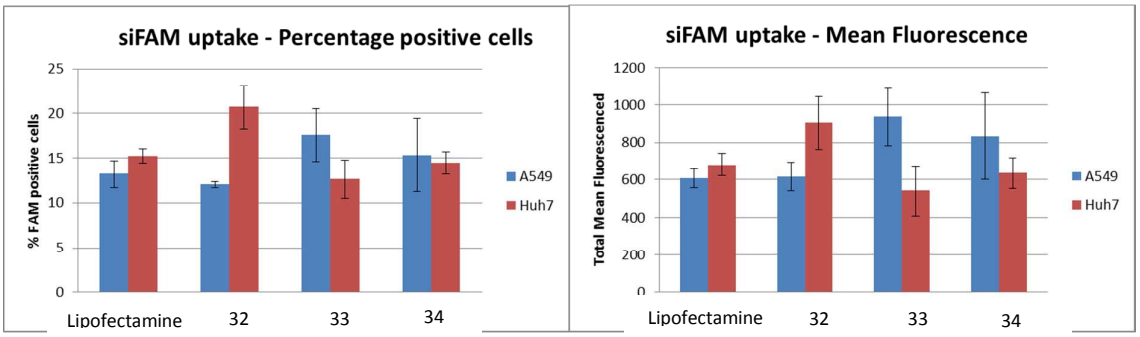

Figure 7: Fluorescent siRNA uptake **(A)** Percentage of cells positive for fluorescent siRNA; **(B)** Mean siRNA fluorescence; Samples were added to cells for 4 h, after which the cells were washed with FACS buffer, trypsinised and analysed on a BD LSRII flow cytometer for FAM fluorescence.

CONCLUSIONS

We have described the synthesis of block copolymers, specifically designed to protect (HPMA section), carry (DMAEMA section) and target (galactose section) ASGP-R-containing liver cells to deliver siRNA. Our systematic approach of post-polymerisation modification enabled a direct comparison of the activity of each polymer and the effect of subtle differences in PEG-linker length and targeting group. Interestingly, no significant difference in siRNA binding or GFP knockdown was observed between quaternised and unquaternised polymers. Disappointingly, no difference in uptake between galactose- and control glucose-functionalised polymers in non-hepatic A549 cells and hepatic Huh7 cells

was observed. Multiple endocytosis mechanisms are active in all cells. These include phagocytosis, receptor or clathrin mediated endocytosis, caveolin mediated endocytosis, lipid-raft enabled endocytosis and macropinocytosis. The mechanism which is used by a cell is determined by a variety of characteristics, most importantly size, shape, charge and ligand recognition.[44-45] Phagocytosis is dominant primarily for non-specific large particles (200-1000 nm), whereas macropinocytosis is dominant for non-specific uptake of smaller (10-200 nm) particles. Both lipid rafts and clathrin mediated endocytosis are specific for ligands on proteins generally between 40-100 nm in size. Depending on the uptake pathways most nanoparticles are transported to endosomes, although this can result in significantly different cell localisation. As previously published, the ABA triblock without galactose forms a nanoparticle of 20-40 nm in diameter which may be too small for efficient clathrin mediated endocytosis uptake.[29] As surmised by the Reineke group, the large cationic carrier block may therefore promote non-ligand dependent uptake mechanisms, which would swamp the effect of the carbohydrate targeting groups. Physicochemical analysis of these particles may shed some light on this. At low N:P ratios our ABA galactose polymers failed to display GFP knockdown in CHO-GFP cells, or cell death in A549 cells or significant cell death in Huh7 cells - observations consistent with the conclusion that the ABA triblock system may prevent release of siRNA in the endosome. Investigations into novel, non-linear constructs containing ASGPR-targeting functionality are underway, to gain a better understanding of endocytotic release of siRNA from the cationic carrier block, and how targeting functionality can be incorporated to maximise ASGPR interactions and, ultimately, cellular uptake.

REFERENCES

1. Hannon, G. J., RNA interference. *Nature* **2002,** *418* (6894), 244-51.
2. Elbashir, S. M.; Harborth, J.; Lendeckel, W.; Yalcin, A.; Weber, K.; Tuschl, T., Duplexes of 21-nucleotide RNAs mediate RNA interference in cultured mammalian cells. *Nature* **2001,** *411* (6836), 494-8.
3. Koutsilieri, E.; Rethwilm, A.; Scheller, C., The therapeutic potential of siRNA in gene therapy of neurodegenerative disorders. *Journal of Neural Transmission-Supplement* **2007,** (72), 43-49.
4. Seth, S.; Johns, R.; Templin, M. V., Delivery and biodistribution of siRNA for cancer therapy: challenges and future prospects. *Ther Deliv* **2012,** *3* (2), 245-61.
5. Weinberg, M. S.; Arbuthnot, P., Progress in the use of RNA interference as a therapy for chronic hepatitis B virus infection. *Genome Medicine* **2010,** *2*.
6. Stanton, M. G.; Colletti, S. L., Medicinal Chemistry of siRNA Delivery. *Journal of Medicinal Chemistry* **2010,** *53* (22), 7887-7901.
7. Oliveira, S.; Storm, G.; Schiffelers, R. M., Targeted delivery of siRNA. *Journal of Biomedicine and Biotechnology* **2006**.
8. Chu, D. S. H.; Schellinger, J. G.; Shi, J. L.; Convertine, A. J.; Stayton, P. S.; Pun, S. H., Application of Living Free Radical Polymerization for Nucleic Acid Delivery. *Accounts of Chemical Research* **2012,** *45* (7), 1089-1099.
9. Bruno, K., Using drug-excipient interactions for siRNA delivery. *Advanced Drug Delivery Reviews* **2011,** *63* (13), 1210-1226.
10. Cheung, S. T.; Tsui, T. Y.; Wang, W. L.; Yang, Z. F.; Wong, S. Y.; Ip, Y. C.; Luk, J.; Fan, S. T., Liver as an ideal target for gene therapy: Expression of CTLA4Ig by retroviral gene transfer. *Journal of Gastroenterology and Hepatology* **2002,** *17* (9), 1008-1014.
11. Shim, G.; Lee, S.; Choi, H.; Lee, J.; Kim, C.-W.; Byun, Y.; Oh, Y.-K., Nanomedicines for Receptor-Mediated Tumor Targeting. *Recent Patents on Nanomedicine* **2011,** *1* (2), 138-148.
12. Kopecek, J.; Kopeckova, P., HPMA copolymers: Origins, early developments, present, and future. *Advanced Drug Delivery Reviews* **2010,** *62* (2), 122-149.
13. Nair, J. K.; Willoughby, J. L. S.; Chan, A.; Charisse, K.; Alam, M. R.; Wang, Q. F.; Hoekstra, M.; Kandasamy, P.; Kel'in, A. V.; Milstein, S.; Taneja, N.; O'Shea, J.; Shaikh, S.; Zhang, L. G.; van der Sluis, R. J.; Jung, M. E.; Akinc, A.; Hutabarat, R.; Kuchimanchi, S.; Fitzgerald, K.; Zimmermann, T.; van Berkel, T. J. C.; Maier, M. A.; Rajeev, K. G.; Manoharan, M., Multivalent N-Acetylgalactosamine-Conjugated siRNA Localizes in Hepatocytes and Elicits Robust RNAi-Mediated Gene Silencing. *Journal of the American Chemical Society* **2014,** *136* (49), 16958-16961.
14. Lee, Y. C.; Lee, R. T.; Ernst, B.; Hart, G. W.; Sinaý, P., Interactions of Oligosaccharides and Glycopeptides with Hepatic Carbohydrate Receptors. In *Carbohydrates in Chemistry and Biology*, Wiley-VCH Verlag GmbH: 2008; pp 549-561.
15. Huang, Y. Y., Preclinical and Clinical Advances of GalNAc-Decorated Nucleic Acid Therapeutics. *Molecular Therapy-Nucleic Acids* **2017,** *6*, 116-132.
16. Dicerna, Welcome to Investor Day. 2016.
17. Lee, R. T.; Lee, Y. C., Affinity enhancement by multivalent lectin-carbohydrate interaction. *Glycoconjugate Journal* **2000,** *17* (7-9), 543-551.
18. Khorev, O.; Stokmaier, D.; Schwardt, O.; Cutting, B.; Ernst, B., Trivalent, Gal/GalNAc-containing ligands designed for the asialoglycoprotein receptor. *Bioorganic & Medicinal Chemistry* **2008,** *16* (9), 5216-5231.
19. Dhande, Y. K.; Wagh, B. S.; Hall, B. C.; Sprouse, D.; Hackett, P. B.; Reineke, T. M., N-Acetylgalactosamine Block-co-Polycations Form Stable Polyplexes with Plasmids and Promote Liver-Targeted Delivery. *Biomacromolecules* **2016,** *17* (3), 830-840.
20. Jiang, H. L.; Kwon, J. T.; Kim, E. M.; Kim, Y. K.; Arote, R.; Jere, D.; Jeong, H. J.; Jang, M. K.; Nah, J. W.; Xu, C. X.; Park, I. K.; Cho, M. H.; Cho, C. S., Galactosylated poly(ethylene glycol)-chitosan-graft-

polyethylenimine as a gene carrier for hepatocyte-targeting. *Journal of Controlled Release* **2008,** *131* (2), 150-157.
21. Thapa, B.; Kumar, P.; Zeng, H. B.; Narain, R., Asialoglycoprotein Receptor-Mediated Gene Delivery to Hepatocytes Using Galactosylated Polymers. *Biomacromolecules* **2015,** *16* (9), 3008-3020.
22. Biessen, E. A. L.; Beuting, D. M.; Roelen, H.; Vandemarel, G. A.; Vanboom, J. H.; Vanberkel, T. J. C., SYNTHESIS OF CLUSTER GALACTOSIDES WITH HIGH-AFFINITY FOR THE HEPATIC ASIALOGLYCOPROTEIN RECEPTOR. *J Med Chem* **1995,** *38* (9), 1538-1546.
23. Diaz-Dussan, D.; Nakagawa, Y.; Peng, Y. Y.; Sanchez, C. L. V.; Ebara, M.; Kumar, P.; Narain, R., Effective and Specific Gene Silencing of Epidermal Growth Factor Receptors Mediated by Conjugated Oxaborole and Galactose-Based Polymers. *Acs Macro Letters* **2017,** *6* (7), 768-774.
24. Managit, C.; Kawakami, S.; Yamashita, F.; Hashida, M., Effect of galactose density on asialoglycoprotein receptor-mediated uptake of galactosylated liposomes. *Journal of Pharmaceutical Sciences* **2005,** *94* (10), 2266-2275.
25. De Smedt, S. C.; Demeester, J.; Hennink, W. E., Cationic polymer based gene delivery systems. *Pharmaceutical Research* **2000,** *17* (2), 113-126.
26. Chiefari, J.; Chong, Y. K.; Ercole, F.; Krstina, J.; Jeffery, J.; Le, T. P. T.; Mayadunne, R. T. A.; Meijs, G. F.; Moad, C. L.; Moad, G.; Rizzardo, E.; Thang, S. H., Living free-radical polymerization by reversible addition-fragmentation chain transfer: The RAFT process. *Macromolecules* **1998,** *31* (16), 5559-5562.
27. Moad, G.; Rizzardo, E.; Thang, S. H., Living radical polymerization by the RAFT process. *Australian Journal of Chemistry* **2005,** *58* (6), 379-410.
28. Moad, G.; Rizzardo, E.; Thang, S. H., Toward living radical polymerization. *Accounts of Chemical Research* **2008,** *41* (9), 1133-1142.
29. Hinton, T. M.; Guerrero-Sanchez, C.; Graham, J. E.; Le, T.; Muir, B. W.; Shi, S. N.; Tizard, M. L. V.; Gunatillake, P. A.; McLean, K. M.; Thang, S. H., The effect of RAFT-derived cationic block copolymer structure on gene silencing efficiency. *Biomaterials* **2012,** *33* (30), 7631-7642.
30. Gao, H. F.; Matyjaszewski, K., Synthesis of molecular brushes by "grafting onto" method: Combination of ATRP and click reactions. *Journal of the American Chemical Society* **2007,** *129* (20), 6633-6639.
31. Ladmiral, V.; Mantovani, G.; Clarkson, G. J.; Cauet, S.; Irwin, J. L.; Haddleton, D. M., Synthesis of neoglycopolymers by a combination of "click chemistry" and living radical polymerization. *Journal of the American Chemical Society* **2006,** *128* (14), 4823-4830.
32. Engler, A. C.; Lee, H. I.; Hammond, P. T., Highly Efficient "Grafting onto" a Polypeptide Backbone Using Click Chemistry. *Angewandte Chemie-International Edition* **2009,** *48* (49), 9334-9338.
33. Tang, H. Y.; Zhang, D. H., General Route toward Side-Chain-Functionalized alpha-Helical Polypeptides. *Biomacromolecules* **2010,** *11* (6), 1585-1592.
34. Han, J.; Li, S. P.; Tang, A. J.; Gao, C., Water-Soluble and Clickable Segmented Hyperbranched Polymers for Multifunctionalization and Novel Architecture Construction. *Macromolecules* **2012,** *45* (12), 4966-4977.
35. Sumerlin, B. S.; Tsarevsky, N. V.; Louche, G.; Lee, R. Y.; Matyjaszewski, K., Highly efficient "click" functionalization of poly(3-azidopropyl methacrylate) prepared by ATRP. *Macromolecules* **2005,** *38* (18), 7540-7545.
36. Yhaya, F.; Binauld, S.; Kim, Y.; Stenzel, M. H., Shell Cross-linking of Cyclodextrin-Based Micelles via Supramolecular Chemistry for the Delivery of Drugs. *Macromolecular Rapid Communications* **2012,** *33* (21), 1868-1874.
37. Narain, R.; Armes, S. P., Synthesis and aqueous solution properties of novel sugar methacrylate-based homopolymers and block copolymers. *Biomacromolecules* **2003,** *4* (6), 1746-1758.
38. Kobayashi, K.; Sumitomo, H.; Ina, Y., Synthesis and Functions of Polystyrene Derivatives Having Pendant Oligosaccharides. *Polymer Journal* **1985,** *17* (4), 567-575.

39. Cho, C. C.; Liu, J. N.; Chien, C. H.; Shie, J. J.; Chen, Y. C.; Fang, J. M., Direct amidation of aldoses and decarboxylative amidation of alpha-keto acids: an efficient conjugation method for unprotected carbohydrate molecules. *Journal of Organic Chemistry* **2009,** *74* (4), 1549-56.
40. Macdonald, J. E.; Kelly, J. A.; Veinot, J. G. C., Iron/Iron oxide nanoparticle sequestration of catalytic metal impurities from aqueous media and organic reaction products. *Langmuir* **2007,** *23* (19), 9543-9545.
41. Adler, A. F.; Leong, K. W., Emerging links between surface nanotechnology and endocytosis: Impact on nonviral gene delivery. *Nano Today* **2010,** *5* (6), 553-569.
42. Dearnley, M.; Reynolds, N. P.; Cass, P.; Wei, X. H.; Shi, S. N.; Mohammed, A. A.; Le, T.; Gunatillake, P.; Tizard, M. L.; Thang, S. H.; Hinton, T. M., Comparing Gene Silencing and Physiochemical Properties in siRNA Bound Cationic Star-Polymer Complexes. *Biomacromolecules* **2016,** *17* (11), 3532-3546.
43. Mingozzi, F.; High, K. A., Therapeutic in vivo gene transfer for genetic disease using AAV: progress and challenges. *Nature Reviews Genetics* **2011,** *12* (5), 341-355.
44. Zauner, W.; Farrow, N. A.; Haines, A. M. R., In vitro uptake of polystyrene microspheres: effect of particle size, cell line and cell density. *Journal of Controlled Release* **2001,** *71* (1), 39-51.
45. Petros, R. A.; DeSimone, J. M., Strategies in the design of nanoparticles for therapeutic applications. *Nature Reviews Drug Discovery* **2010,** *9* (8), 615-627.